NH_3-efficient ammoxidation of toluene by hydrothermally synthesized layered tungsten-vanadium complex metal oxides

Yoshinori Goto,[a] Ken-ichi Shimizu,*[a,b] Kenichi Kon,[a] Takashi Toyao,[a,b] Toru Murayama,[a, c] Wataru Ueda*[d]

[a] Institute for Catalysis, Hokkaido University, N-21, W-10, Sapporo 001-0021, Japan
[b]Elements Strategy Initiative for Catalysts and Batteries, Kyoto University, Katsura, Kyoto 615-8520, Japan
[c]Research Center for Gold Chemistry, Graduate School of Urban Environmental Sciences, Tokyo Metropolitan University, 1-1 Minami-osawa, Hachioji, Tokyo 192-0397, Japan
[d]Kanagawa University, Rokkakubashi 3-27-1, Yokohama 221-8686, Japan

*Corresponding author: E-mail: uedaw@kanagawa-u.ac.jp, kshimizu@cat.hokudai.ac.jp

Abstract

Hydrothermally synthesized W–V-O layered metal oxides (W–V–O) are studied for the vapor phase ammoxidation of toluene to benzonitrile (PhCN). Under similar conversion levels at 400 ˚C, W–V–O shows higher selectivity (based on toluene) to PhCN and lower selectivity to COx than conventional V-based catalysts (V_2O_5 and VO_x/TiO_2). Under the conditions of high contact time, W-V-O shows 99.7% conversion of toluene and 93.5% selectivity to PhCN. Another important feature of W–V–O is high NH_3-utilization efficiency in ammoxidation, which originates from the lower activity of W–V–O for NH_3 oxidation than that of V_2O_5. In situ infrared (IR) study shows that toluene is oxidized by the surface oxygen species of W83V17 to yield benzaldehyde which undergoes the reaction with adsorbed NH_3 to give benzonitrile. Model reaction studies with W–V–O suggest that the rate of NH_3 conversion to PhCN in the benzaldehyde+NH_3+O_2 reaction is 3 times higher than the rate of NH_3 oxidation to N_2 in the NH_3+O_2 reaction. It is shown that the high NH_3-efficiency of W-V-O is caused by the preferential reaction of NH_3 in PhCHO+NH_3+O_2 over NH_3+O_2 reaction.

1. Introduction

Ammoxidation of methyl-substituted aromatics such as toluene, xylene and methylpyridine to their corresponding nitriles is an industrially important reaction, and numerous reports have been dealt with this reaction [1-4]. The vapor phase ammoxidation of toluene to benzonitrile has been extensively studied as a model reaction [5-16]. Various metal oxide-based catalysts, including vanadium (V)-based catalysts (V_2O_5 [5], VO_x/TiO_2 [6,7], VO_x/ZrO_2 [8], V_2O_5/Nb_2O_5-TiO_2 [9], $(VO)_2P_2O_7$ [10-13]) and other catalysts (MoO_x/Nb_2O_5 [13], MoO_x/ZrO_2

[15], Fe-based mixed oxides [16]) have been reported to show moderate to good yields (44-77%) of benzonitrile (based on toluene) at around 400 ˚C [5-16]. The catalytic efficiency in the ammoxidation of toluene has been discussed in terms of the selectivity or yield of benzonitrile based on toluene. In addition to the non-selective oxidation of toluene to COx, another undesired side-reaction in the ammoxidation is non-selective oxidation of ammonia (NH_3) to N_2. In order to establish a sustainable ammoxidation process, NH_3 consumption during the reaction should also be minimized. However, quite a few reports have discussed the benzonitrile selectivity based on the NH_3 consumed, or in other words, the efficiency of NH_3 utilization in ammoxidation of benzonitrile. Mechanistic studies on vanadium oxides-catalyzed ammoxidation of toluene [6,7,11-13] suggested bifunctional catalysis as a catalyst design concept. It is proposed that the VO_x sites catalyze partial oxidation of toluene to benzaldehyde-like intermediate and acid sites act as adsorption site of NH_3 [3,11-13]. If one designed a V-based mixed oxide catalyst having NH_3 adsorption sites (such as acidic WOx sites) in close proximity to the redox sites (VOx), the aldehyde intermediate formed on the redox site would have react preferentially with NH_3 on the acid site, resulting in high efficiency of NH_3 utilization in the ammoxidation reaction.

Our research group has focused on the hydrothermal synthesis of single crystalline Mo-V-O based catalysts [17-19]. Particularly, single phasic orthorhombic Mo_3VO_x, having a microporous and layered structure, is of importance because its structure is basically the same as that of so called “M1 phase” which is well known as active phase in the industrial selective oxidation catalysts [18]. We have found that the Mo-V-O catalysts, as a structurally well defined catalytic phase for “M1 phase”, catalyzed the selective oxidative dehydrogenation of ethane at low temperature (300 ˚C) [18]. The single phase Mo-V-P catalyst with similar structure also catalyzed the ammoxidation of propane [19]. Recently, we have extended the hydrothermal synthetic methodology to metal oxides consisted of various group 5 and 6 elements [20-23], and prepared a series of binary metal oxides (such as W-Ta-O [20,23], W-Nb-O [21] and W-V-O complex oxides [22]) with similar microporous and layered structure as the orthorhombic Mo_3VO_x [18]. Considering the fact that WOx is an well known acidic co-catalyst of V-based catalysts [24-27], we have hypothesized that the W-V-O oxides act as effective catalysts for the ammoxidation. In this regard, we have recently reported the W-V-O-catalyzed highly selective ammoxidation of 3-picoline to 3-cyanopyridine [22]. We report herein a highly selective gas-phase ammoxidation of toluene by the hydrothermally prepared W-V-O layered oxides. The catalysts show high efficiency of NH_3 utilization in ammoxidation as well as high selectivity of benzonitrile based on toluene. In situ IR study shows that the reaction of benzaldehyde with NH_3 is a main pathway to benzonitrile on this

catalytic system. Model reaction studies are also conducted to discuss the reason why the W-V-O catalyst shows high efficiency of NH_3 utilization.

2. Experimental

2.1. Catalyst preparation

Inorganic materials were purchased from Wako Pure Chemical Industries. According to our previous report [22], the complex metal oxide of W and V (W-V-O) with W/V molar ratio of 83/17, named W83V17, was prepared by a hydrothermal synthesis method as follows. An aqueous solution (40 mL) of $(NH_4)_6[H_2W_{12}O_{40}]\cdot nH_2O$ (10.4 mmol), $VOSO_4\cdot nH_2O$ (4.16 mmol) and oxalic acid (0.10 mmol) was introduced into a stainless steel autoclave with a Teflon inner tube (50 mL), followed by filling the inner space of the tube by Teflon thin sheet (50 mm×1000 mm). Then, N_2 (20 mL min^{-1}) was fed into the solution for 10 min to remove residual oxygen. The autoclave attached to a rotating machine was installed in an oven, and the mixture underwent hydrothermal reaction at 175 ˚C for 24 h under mechanical rotation (1 rpm). The solid formed was filtered, washed with ion-exchanged water (1 L), dried at 80 ˚C overnight and then heated at 400 ˚C for 2 h under N_2 flow. W64V36 with W/V molar ratio of 64/36 was prepared according to the method in our previous study [22.] Bulk composition of the catalysts (Table 1) was determined by an inductively coupled plasma (ICP-AES) method (ICPE-9000, Shimadzu). Na^+-exchanged W83V17 (designated as Na-W83V17) was prepared by mixing W-V-O (2.0 g) with 100 mL of aqueous solution of Na_2SO_4 (19.1 mmol) for 5 h at room temperature, followed by centrifuging and washing with ion-exchanged water four times, drying at 80 ˚C overnight and by heating at 400 ˚C for 2 h under N_2 flow. The Na content in Na-W83V17 (0.74 mmol g^{-1}) was determined by ICP-AES analysis. WO_3-supported vanadia (VO_x/WO_3) with W/V molar ratio of 85/15 was prepared by impregnation method; a suspension of WO_3 (20.0 mmol) in an aqueous solution (50 mL) of NH_4VO_3 (3.5 mmol) was heated to 90 ˚C for 30 min to evaporate water, followed by drying at 80 ˚C overnight, and by heating at 400 ˚C for 2 h under N_2 flow. The bulk compositions and surface area of the W-V-O and VO_x/WO_3 catalysts are listed in Table 1. V_2O_5 and WO_3 for catalytic studies were commercially supplied from Wako Pure Chemical Industries. Vanadia loaded TiO_2 with V loading of 5.9 wt%, named VO_x/TiO_2, was prepared by impregnation method [22]; a suspension of anatase TiO_2 (4 g, Wako Pure Chemical Industries) in aqueous oxalic acid solution (50 mL) of NH_4VO_3 (4.9 mmol) was evaporated at 50 ˚C, followed by drying at 100 ˚C, and by heating at 450 ˚C for 6 h under air.

2.2. Catalyst characterization

The BET surface areas of the catalysts were determined by N_2 adsorption at -196 ˚C using BELCAT (MicrotracBEL). Prior to the measurement, the samples were heated under He flow at

400 ˚C for 1 h. Powder X-ray diffraction (XRD) pattern of the catalysts were recorded on a Rigaku MiniFlex II/AP diffractometer with Cu Kα radiation. Scanning electron microscope (SEM) images were taken using a JEOL JSM-7400F field emission scanning electron microscope.

The pyridine-adsorption infrared (IR) spectra were measured at 100 ^{o}C by a JASCO FT/IR-4200 spectrometer equipped with an MCT detector. The IR disc (38±1 mg, ϕ = 2 cm) of a catalyst in the flow-type IR cell. (CaF_2 windows), connected to a flow system, was first dehydrated under He flow (30 cm^3 min^{-1}) at 500 °C for 0.5 h, followed by cooling to the measurement temperature under He. For the adsorption of organic compounds, 0.3 mmol g_{cat}^{-1} of liquid pyridine, toluene, benzaldehyde or benzonitrile was injected to the He flow preheated at 200 °C, and the vaporized organic compound was fed to the IR cell. For the adsorption of NH_3, NH_3(2%)/He (50 cm^3 min^{-1}) was fed to the sample. Then, the IR disk was purged with He for 600 s, and IR measurement was carried out. Spectra were measured accumulating 15 scans at a resolution of 4 cm^{-1}. A reference spectrum of the catalyst wafer in He taken at the measurement temperature was subtracted from each spectrum.

2.3. Catalytic reactions

Vapor phase ammoxidation of toluene was carried out at atmospheric pressure using a fixed-bed flow reactor (Pyrex glass tube) with an inner diameter of 9 mm. Catalyst powders were pressed to pellets, crushed, and sieved. To maintain a constant reaction temperature, the catalyst pellets (0.25-0.50 mm size; typically 1.5 g (1.1 cm^3) of W83V17) were diluted with quartz (0.2-0.4 mm size; 1.5 cm^3) to fill the reactor (2.6 cm^3). Use of the same volume (2.6 cm^3) of the pellets with the same size range will result in the same pressure drop for different catalyst loadings. The reaction temperature was measured inside the catalyst bed by a thermocouple, whose tip was inside the upper side of the catalyst bed. The gas stream (NH_3/O_2/He) was fed to the reactor with mass flow controllers. Toluene was fed continuously into the gas stream at 150 ˚C from a syringe pump with a micro-feeder. The reactor was fed with toluene/NH_3/O_2/He mixture in the molar ratio of 1/10/4/34 with total flow rate (F) of 49 mL min^{-1}. Under the low NH_3 concentration conditions in Fig. 7, the molar ratio of toluene/NH_3/O_2/He was 1/5/4/39 (F = 49 mL min^{-1}). CH_4 was fed into outlet gas as external standard for GC-TCD analysis.

As a model reaction (Fig. 9), benzaldehyde+NH_3+O_2 reaction by 0.1 g of the catalyst, diluted with the quartz pellets (2.5 cm^3), was carried out with the same reactor which was fed with benzaldehyde/NH_3/O_2/He mixture in the molar ratio of 1/10/4/34 (F = 49 mL min^{-1}). A model reaction (Fig. 9) of NH_3+O_2 by 0.1 g of the catalyst was carried out using NH_3/O_2/He mixture in the molar ratio of 10/4/35 (F = 49 mL min^{-1}).

The gas phase products (CO, CO_2 and N_2) in the outlet gas were analyzed by GC-TCD (GL

Sciences GC-3200, 6 m SHINCARBON-ST packed column). Organic products, trapped in ethanol at 0 ˚C, followed by adding *n*-octane as an external standard, were analyzed with GC-FID (Shimadzu GC-14B with TC-5 capillary column). The carbon balance values for all the catalytic results were in a range of 95.9-101.6%.

For the ammoxidation of toluene in the present system, the nitrogen containing products were N_2 and benzonitrile (PhCN) with very small amount of benzamide (amide). GC-TCD analysis showed no formation of N_2O. Thus, the efficiency of NH_3 utilization in ammoxidation (η_{NH3}) is defined as

$$\eta_{NH3} = y_{PhCN} n_{PhCN} / (y_{PhCN} n_{PhCN} + y_{amide} n_{amide} + y_{N2N} n_{N2}),$$

where y_{PhCN}, y_{amide} and y_{N2} are the molar amounts of nitrogen containing products, and n_{PhCN}, n_{amide} and n_{N2} are the number of nitrogen atoms in each product.

3. Result and discussion

3.1. Catalyst characterization

In our recent report [22], we synthesized a W-V-O catalyst with W/V ratio of 67/33 and studied its structure by various characterization methods: XRD, scanning transmission electron microscopy (STEM) and N_2-adsorption isotherm. Briefly, the results showed three structural features: (i) layered-type structure along *c*-axis direction characterized by diffraction peaks at 2θ = 23° and 46° (XRD), (ii) long rod-shaped crystal morphology due to stacking of the layers along the *c*-axis by sharing the apex oxygen (STEM), (iii) the presence of micropore (N_2-adsorption). Considering the structural model that we have proposed for the similar binary metal oxides consisted of group 5 and 6 elements [17-23], the structural model of W-V-O is proposed in Fig. 1. In this paper, W-V-O catalysts with different compositions (W64V36 and W83V17) were prepared. As shown in Fig. 1, their XRD patterns have essentially the same feature: two sharp diffraction peaks around 23° and 46° assignable to the (0 0 1) and (0 0 2) planes of the layered structure along *c*-axis direction. The XRD pattern of Na-W83V17 also has the same diffraction peaks at 23° and 46°. Although the intensities of Na-W83V17 are lower than those of W83V17, the XRD results indicate that the Na^+-exchanged W83V17 (Na-W83V17) has basically the same crystal structure as W83V17. The SEM image of W83V17 (Fig. 2) showed the rod-shaped crystal probably due to stacking of the layers along the *c*-axis. Before calcination of the hydrothermally prepared binary metal oxides NH_4^+ is located in the 6 and 7-membered ring pores, and thermal desorption of NH_3 from the precursor results in the formation of Brønsted acid sites in the pores [18]. The proton is exchangeable to various cations in aqueous solution [18].

Fig. 3 shows IR spectra (the ring-stretching region) of pyridine adsorbed on W83V17 and Na-W83V17. The spectrum for W83V17 shows the adsorption band at 1536 cm^{-1} due to

pyridinium ion (PyH^+) produced by the reaction of pyridine with Brønsted acid sites and the adsorption band at 1447 cm^{-1} due to coordinatively bound pyridine on Lewis acid sites [28]. The results indicate that the surface of W83V17 has both Brønsted and Lewis acid sites. Note that the weight of the catalyst disc for the IR experiment was the same for different catalysts, so the differences in the peak area at 1536 cm^{-1} and at 1447 cm^{-1} between samples corresponds to the difference in the amount of Brønsted and Lewis acid sites. The spectrum for Na-W83V17 shows lower intensities of these bands, which indicates that the H^+/Na^+ cation exchange results in decrease in the number of Brønsted and Lewis acid sites of W83V17. It should be noted that the results of XRD show that the crystal structures of Na-W83V17 and W83V17 are similar to each other, and the surface area (Table 1) of Na-W83V17 (38.5 $m^2\ g^{-1}$) is close to that of W83V17 (41.9 $m^2\ g^{-1}$). These results indicate that the structure of W83V17 is essentially very close to that of Na-W83V17 except for acidity; W83V17 has larger amount of Brønsted and Lewis acid sites than Na-W83V17. The result also shows that W83V17 has larger amount of Brønsted and Lewis acid sites than V_2O_5.

3.2. Catalytic performance

Fig. 4 shows the effects of contact time on the properties of ammoxidation by W83V17 at 400 ˚C. Experiments were carried out by changing the catalyst weight (0.15, 0.75, 1.9, 1.5, 2.0 g) with the same inlet gas flow rate. The conversion of toluene increased with the contact time. The increase in the conversion resulted in slight decrease in the selectivity to benzonitrile (S_{PhCN}) and slight increase in the COx selectivity (S_{COx}). The selectivities to benzamide (S_{amide}) were below 0.9%. Hence, NH_3 can be consumed by two of the competitive reactions: (1) ammoxidation with toluene to produce benzonitrile and (2) NH_3 oxidation to N_2. Interestingly, the increase in the contact time resulted in the increase in the NH_3-efficiency (η_{NH3}). This indicates a preferential promotion of the ammoxidation by W83V17 over the non-selective NH_3 oxidation.

We tested various V-based catalysts (1.5 g of W83V17, W64V36, Na-W83V17, VO_x/WO_3 and WO_3 and 0.5 g of V_2O_5) for the ammoxidation of toluene. To compare the selectivities of V_2O_5 and W-V complex oxide catalysts under the similar conversion levels, the catalyst amount of V_2O_5 was decreased. For representative catalysts, the effects of temperature on the toluene conversion, selectivity to various products and NH_3-efficiency are plotted in Fig. 5. Under the similar conversion levels, W83V17 showed higher selectivity to benzonitrile (S_{PhCN}) than the conventional V-based catalysts (V_2O_5 and VO_x/TiO_2). V_2O_5 and VO_x/TiO_2 showed higher selectivity to COx than W83V17.

Table 2 compares the conversions of toluene and selectivities to benzonitrile (S_{PhCN}), benzamide (S_{amide}), benzoic acid (S_{acid}), benzene (S_{Bz}) and COx (S_{COx}) at 400°C. A conventional

catalyst, V_2O_5, showed 71.2% selectivity to benzonitrile at a conversion level of 87.2%. WO_3 showed only 9.2% conversion of toluene. This indicates that vanadium is an indispensable element for this catalytic system. W83V17, W64V36 and VO_x/WO_3 show higher selectivities to benzonitrile than V_2O_5. This indicates that tungsten oxides as co-catalysts increase the selectivity to benzonitrile. The hydrothermally prepared catalysts (W83V17 and W64V36) showed higher selectivity to benzonitrile than VO_x/WO_3. Na-W83V17 showed low conversion (12.6%) than W83V17 (85.1%). Combined with the IR results in Fig. 3, we can conclude that Brønsted and/or Lewis acid sites of W83V17 significantly improve the ammoxidation activity in the present system.

Another remarkable feature of the hydrothermally prepared W-V-O catalysts (W83V17, W64V36) is highly efficient utilization of NH_3 in ammoxidation. The results in Fig. 5 and Table 2 demonstrated that W83V17 showed high NH_3-efficiency (η_{NH3}) than other V-based catalysts. As shown in Table 2, the order of the NH_3-efficiency (η_{NH3}) of V-based catalysts is as follows: W83V17 (56.9%) ≈ W64V36 (44.8%) > VO_x/TiO_2 (42.2%) > VO_x/WO_3 (36.4%) > V_2O_5 (34.9%). The result indicates that the W-V-O catalysts (W83V17, W64V36) preferentially promote the ammoxidation over the non-selective NH_3 oxidation, while the classical and conventional V-based catalysts show moderate activity for the oxidation of NH_3 to N_2. The catalytic results in Table 2 are converted to the rate of benzonitrile formation per surface area of the catalysts listed in Table 1. The reaction rates for W-V-O catalysts (W83V17, W64V36) are lower than that of V_2O_5. It is obvious that the main advantages of the W-V-O catalysts are high selectivity to benzonitrile (low selectivity to COx) and highly efficient utilization of NH_3.

Most of the previous reports on ammoxidation of toluene adopted excess NH_3 feed conditions. The reaction with lower level of NH_3 feed will lead to more sustainable and economical production of benzonitrile. Fig. 6 shows the results for the W83V17-catalyzed ammoxidation with different the amount of NH_3 (2, 5, 10 and 15 equiv. with respect to toluene). The selectivity to benzonitrile decreased with decreasing NH_3 concentration, but NH_3-efficiency (η_{NH3}) increased with decreasing NH_3 concentration. At the NH_3 molar ratio of 2 equiv. (NH_3/toluene = 2/1), the NH_3-efficiency was 73.9% and the yield of benzonitrile was 70.2%. This indicates that the present system can produce benzonitrile with high NH_3-efficiency and high yield under low NH_3 feed conditions. However, it is important to note that the ammonia levels required for achieving good benzonitrile yields are still several times above that required for the stoichiometric reaction. Further studies are necessary to address this issue.

Fig. 7 shows the catalytic results by 1.5 g of W83V17 and 0.5 g of V_2O_5 for the ammoxidation of toluene with lower NH_3 molar ratio (5 equiv.) than the standard conditions in Fig. 5 (10 equiv.). The general trends were basically similar to those for the standard conditions in Fig. 5, but the difference between W83V17 and V_2O_5 were more significant in Fig. 7. At 440

˚C, where the toluene conversion reached 100% for both catalysts, V_2O_5 showed 52.1% selectivity to benzonitrile and 29.6% of NH_3-efficiency, while W83V17 showed 84.9% selectivity to benzonitrile and 80.5% of NH_3-efficiency. The results clearly demonstrate that W83V17 shows high efficiency of NH_3 utilization in ammoxidation as well as high selectivity to benzonitrile based on toluene. For the reaction with W83V17 at 420 ˚C, the yield of benzonitrile is 85.2 %, corresponding to the benzonitrile productivity of 129 g $L_{\text{-cat}}^{-1}$ h^{-1}. The yield and the productivity of this system are not high compared with the yields (67-92%) and the productivities (52-342 g $L_{\text{-cat}}^{-1}$ h^{-1}) of the benchmark V-based catalysts in the patents for ammoxidation of toluene [1].

Fig. 8 shows the stability versus time-on-stream of W83V17-catalyzed ammoxidation of toluene under the standard conditions at 400 ˚C. The toluene conversion slightly decreased from 98.6% to 95.1% during the 45 h of the continuous reaction. Then, the catalyst was heated at 500 ˚C for 1 h under He flow. The heat-treatment increased the toluene conversion to 97.6%, and the catalytic system showed high conversions (> 95.9%) for the next 30 h. The benzonitrile selectivity (90.2-90.4%) and NH_3-efficiency (50.9-53.1%) were nearly constant throughout the experiment. We also studied the effects of co-feeding of water on the catalytic performance of W83V17. As compared in Table 2, co-feeding of water vapor did not essentially change the toluene conversion, the selectivity to benzonitrile and NH_3-efficiency (η_{NH3}). These results suggest that the present catalytic system is tolerant to water vapor.

3.3. Mechanistic and in situ IR studies

Previous studies [3, 11] on the mechanism of ammoxidation of toluene by V-based catalyst suggest that benzonitrile is produced via a benzaldehyde intermediate, which then reacts with NH_3 on the surface to yield benzylimine surface species. Finally, the benzylimine intermediate undergoes oxidative dehydrogenation to give benzonitrile [3,11]. We carried out a model reaction of benzaldehyde+NH_3+O_2 by W83V17 and V_2O_5 catalysts. The results in Fig. 9 (left) were consistent with the proposed mechanism in the literature [3, 11]; the formation rates of benzonitrile by ammoxidation of benzaldehyde were more than 6 times higher than those by ammoxidation of toluene (right) for both catalysts. This suggests that the ammoxidation of toluene by W83V17 is also driven by the proposed mechanism in the literature [3, 11], eqn. (1), including the partial oxidation of toluene to benzaldehyde as a rate-limiting step.

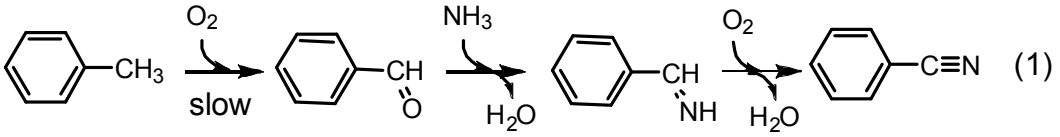

(1)

To verify the hypothetical mechanism, we studied formation and reaction of intermediates on the W83V17 catalyst using in situ IR spectroscopy. First, adsorption of toluene and benzaldehyde was studied in order to identify the adsorbed species that could arise on the surface of W83V17 during the ammoxidation of toluene. Gaseous toluene or benzaldehyde (0.3 mmol $g_{cat.}^{-1}$) was introduced to the flow-type in situ IR cell at various temperatures under He flow, followed by purging with He flow for 600 s to obtain the IR spectra in Fig. 10. The spectrum of toluene adsorbed on W83V17 at ambient temperature showed two ring vibration bands of aromatics (1498 and 1588 cm^{-1}) [29] but no band due to C=O or C-O stretching modes, indicating that toluene was not oxidized by the surface oxygen of W83V17 but physically adsorbed on the surface at ambient temperature. At higher temperature (200 ˚C), a weak band at 1705 cm^{-1} assignable to C=O stretching modes (ν_{CO}) of benzaldehyde [11] and ring vibration bands of aromatics (1498 and 1588 cm^{-1}) were observed. The ν_{CO} band at 1705 cm^{-1} was also observed for benzaldehyde adsorbed on W83V17 at ambient temperature. These results indicate that toluene is oxidized by surface oxygen species of W83V17 to yield benzaldehyde even at lower temperature (200 ˚C) than the reaction temperature (400 ˚C) of the catalytic ammoxidation in this study. In the spectrum of benzonitrile on W83V17, a band at 2262 cm^{-1} due to C≡N stretching modes (ν_{CN}) of adsorbed benzonitrile was observed.

As shown in Fig. 11, the adsorption of NH_3 at 330 ˚C resulted in the formation of IR bands due to protonated ammonia (NH_4^+) on Brønsted acid sites at 1410 cm^{-1} [28] and coordinated ammonia on Lewis acid sites at 1256 cm^{-1} [28]. Then, we studied the reaction of the adsorbed NH_3 species with toluene at 330 ˚C under He flow. Soon after the introduction of gaseous toluene (0.3 mmol g_{cat}^{-1}) to the NH_3-preadsorbed W83V17, the band at 2250 cm^{-1} due to ν_{CN} of benzonitrile was observed, and the intensity of the ν_{CN} band increased with time. The introduction of toluene decreased the intensities of the bands of NH_4^+ (1410 cm^{-1}) and coordinated NH_3 (1256 cm^{-1}). These results indicate that benzonitrile is produced by the reaction of adsorbed NH_3 and toluene with oxygen atoms on the surface of W83V17 at 330 ˚C.

The same NH_3 adsorption experiment for V_2O_5 (Fig. 11B) shows that the amount of adsorbed NH_3 on V_2O_5 is negligible at 330 °C. Comparison of the results for W83V17 and V_2O_5 indicates that the acid sites originate from W in W83V17 act as adsorption sites of NH_3 during the ammoxidation reaction. The same experiment for VOx/WO_3 shows that it shows adsorbed NH_3 mostly on Brønsted acid sites probably on the surface of WO_3. However, the introduction of toluene to the adsorbed NH_3 on VOx/WO_3 did not result in the formation of adsorbed PhCN. Considering the structural difference between the W83V17 (mixed oxide) and VOx/WO_3 (VOx islands supported on WO_3), one could conclude that proximity between W (acid) sites and V (redox) sites is important for the surface reaction between the adsorbed NH_3, toluene and a reactive oxygen atom on the surface to give PhCN.

Fig. 12 shows the reaction of toluene-derived surface species with NH_3 monitored by in situ IR at 200 ˚C. After the observation of the benzaldehyde (1705 cm^{-1}) on W83V17, the flowing gas was switched from He to 2% NH_3/He and the IR spectra were observed as a function of the time of NH_3 flowing at 200 ˚C. The ν_{CN} band of adsorbed benzonitrile species (2256 and 2232 cm^{-1}) appeared, and the intensity of the ν_{CN} band increased with time. Summarizing the IR results in Figs. 10-12, the following pathway is proposed; toluene is oxidized by the surface oxygen species of W83V17 to yield benzaldehyde which undergoes the reaction with adsorbed NH_3 to give benzonitrile possibly via benzylimine. This pathway is consistent with that proposed in the literature [3, 11] shown in eqn. (1).

Fig. 9 compares the reaction rates for benzaldehyde+NH_3+O_2 (left), NH_3+O_2 (center) and toluene+NH_3+O_2 (right) reactions by W83V17 and V_2O_5. From the results in Fig. 9 and the pathway in eqn. (1), the origin of the higher NH_3-efficiency (η_{NH3}) of W83V17 than that of V_2O_5 is explained as follows. For V_2O_5, the rate of NH_3 conversion to PhCN in the benzaldehyde+NH_3+O_2 reaction is 1.5 times higher than the rate of NH_3 oxidation to N_2 in the NH_3+O_2 reaction. For W83V17, the rate of NH_3 conversion to PhCN is 3 times higher than the rate of NH_3 oxidation to N_2. These results indicate that, especially on W83V17, NH_3 consumption in the condensation of benzaldehyde with NH_3 is faster than NH_3 consumption in NH_3 oxidation to N_2. Comparison of Fig. 9 (left) and Fig. 9 (center) shows that, for both catalysts, the presence of benzaldehyde in the feed decreases the rate of the unselective oxidation of NH_3 to N_2. This indicates that ammoxidation of benzaldehyde competes with NH_3 oxidation to N_2 during ammoxidation of toluene. W83V17 showed lower rate of NH_3 oxidation in the NH_3+O_2 reaction than V_2O_5 (Fig. 6, center). From these results, we could conclude that the high NH_3-efficiency of W-V-O for ammoxidation of toluene is caused by the preferential reaction of NH_3 in the ammoxidation of benzaldehyde over NH_3 oxidation to N_2 as illustrated in eqn. (2).

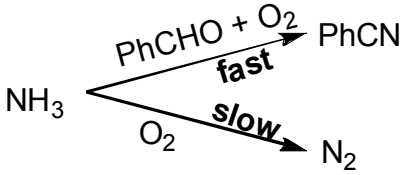

(2)

On the surface of the W-V-O complex oxide, a VO_6 octahedron as a redox site is adjacent to WO_6 octahedra as NH_3 adsorption sites. The benzaldehyde adspecies, once formed by the oxidation of toluene by the VO_6 site, can react preferentially with NH_3 adspecies on the neighboring WO_6 sites, which can result in high efficiency of NH_3 utilization in the present catalytic system.

4. Conclusion

The layered-type W-V-O metal oxides (W-V-O), synthesized by hydrothermal method, selectively catalyzed the gas-phase ammoxidation of toluene to benzonitrile. Under similar conversion levels, W-V-O showed higher selectivity to benzonitrile and lower selectivity to COx than conventional V-based catalysts (V_2O_5 and VO_x/TiO_2). Additionally, W-V-O was less active for the undesired oxidation of NH_3 to N_2, resulting in the high NH_3-utilization efficiency in ammoxidation than the conventional V-based catalysts. W-V-O showed high durability and high tolerance to co-fed water vapor, demonstrating promising catalytic properties of the present system. Model reaction studies suggested that the high NH_3-efficiency of W-V-O was caused by the preferential reaction of NH_3 in PhCHO+NH_3+O_2 over undesired NH_3+O_2 reaction.

References

[1] R.G. Rizayev, E.A. Mamedov, V.P. Vislovskii, V.E. Sheinin, Appl. Catal. A 83 (1992) 103–140.

[2] A. Martin, B. Lücke, Catal. Today 57 (2000) 61–70.

[3] A. Martin, V.N. Kalevaru, ChemCatChem 2 (2010) 1504–1522.

[4] B. Lücke, K. V. Narayana, A. Martin, K. Jähnisch, Adv. Synth. Catal. 346 (2004) 1407–1424.

[5] J.C. Otamiri, A. Andersson, Catal. Today 3 (1988) 211–222.

[6] M. Sanati, A. Andersson, Ind. Eng. Chem. Res. 30 (1991) 312–320.

[7] M. Sanati, A. Andersson, Ind. Eng. Chem. Res. 30 (1991) 320–326.

[8] M. Sanati, A. Andersson, L. R. Wallenberg, B. Rebenstorf, Appl. Catal. A 106 (1993) 51–72.

[9] C.P. Kumar, K.R. Reddy, V.V. Rao, K.V.R. Chary, Green Chem. 4 (2002) 513–516.

[10] A. Martin, F. Hannour, A. Brückner, B. Lücke, React. Kinet. Catal. Lett. 63 (1998) 245–251.

[11] Y. Zhang, A. Martin, H. Berndt, B. Lücke, M. Meisel, J. Mol. Catal. A 118 (1997) 205–214.

[12] A. Martin, B. Lücke, M. Meisel, Top. Catal. 3 (1996) 377–386.

[13] A. Martin, Y. Zhang, H.W. Zanthoff, M. Meisel, M. Baerns, Appl. Catal. A 139 (1996) L11–L16.

[14] K.V.R. Chary, K.R. Reddy, T. Bhaskar, G.V. Sagar, Green Chem. 4 (2002) 206–209.

[15] A. Teimouri, B. Najari, A.N. Chermahini, H. Salavati, M. Fazel-Najafabadi, RSC Adv. 4 (2014) 37679–37686

[16] E. Rombi, I. Ferino, R. Monaci, C. Picciau, V. Solinas, R. Buzzoni, Appl. Catal. A 266 (2004) 73–79.

[17] M. Sadakane, N. Watanabe, T. Katou, Y. Nodasaka, W. Ueda, Angew. Chem. Int. Ed. 46 (2007) 1493–1496.

[18] S. Ishikawa, W. Ueda, Catal. Sci. Technol. 6 (2016) 617–387.

[19] N. Watanabe, W. Ueda, Ind. Eng. Chem. Res. 45 (2006) 607–614.
[20] T. Murayama, N. Kuramata, S. Takatama, K. Nakatani, S. Izumi, X. Yi, W. Ueda, Catal. Today 185 (2012) 224–229.
[21] K. Omata, S. Izumi, T. Murayama, W. Ueda, Catal. Today, 201 (2013) 7–11.
[22] Y. Goto, K. Shimizu, T. Murayama, W. Ueda, Appl. Catal. A 509 (2016) 118–122.
[23] T. Murayama, N. Kuramata, W. Ueda, J. Catal. 339 (2016) 143–152.
[24] M.D. Soriano, P. Concepcion, J.M. Lopez Nieto, F. Cavani, S. Guidetti, C. Trevisanut, Green Chem. 13 (2011) 2954–2962.
[25] A. Chieregato, F. Basile, P. Concepción, S. Guidetti, G. Liosi, M.D. Soriano, C. Trevisanut, F. Cavani, J.M.L. Nieto, Catal. Today 197 (2012) 58.
[26] M.D. Soriano, A. Chieregato, S. Zamora, F. Basile, F. Cavani, J. M. L. Nieto, Top Catal. 59 (2016) 178–185.
[27] X. Li, Y. Zhang, ACS Catal. 6 (2016) 143−150.
[28] M. Tamura, K. Shimizu and A. Satsuma, Appl. Catal. A 433–434 (2012) 135–145.
[29] G. Busca, J. Chem. Soc. Faraday Trans. 89 (1993) 753–755.

Table 1 Surface area, composition and reaction rates of the catalysts.

Catalyst	S[a] (m^2g^{-1})	W/V [b]	V [c] (mmol h^{-1} g^{-1})	V [d] (mmol h^{-1} m^{-2})
W64V36	27.7	64/36	1.51	0.055
W83V17	41.9	83/17	1.40	0.031
Na-W83V17	38.5	83/17	1.29	0.005
VOx/WO_3	14.2	85/15	1.12	0.041
V_2O_5	4.8	-	3.03	0.631
WO_3	16.8	-	0.09	0.003

a BET surface area determined by N_2 adsorption

b Composition determined by ICP-AES

c Rate of BN formation per weight of the catalysts.

d Rate of BN formation per surface area of the catalysts.

Table 2 Catalytic results at 400 ˚C under the conditions in Fig. 5.

Catalyst	Cat. wt. (g)	Conv. (%)	S_{PhCN} (%)	S_{amide} (%)	S_{acid} (%)	S_{Bz} (%)	S_{COx} (%)	η_{NH3} (%)
W83V17	1.5	85.1	93.6	0.9	0	0	5.5	56.9
W83V17[a]	1.5	83.3	93.4	1.5	0	0	5.1	56.0
Na-W83V17	1.5	12.6	99.1	0	0	0	0.9	15.4
W64V36	1.5	99.9	93.0	0.3	0	0.1	6.6	44.8
VOx/WO_3	1.5	83.9	82.5	2.1	0	0	15.4	36.4
VOx/TiO_2	1.0	92.5	76.2	0.8	1.3	1.1	20.6	42.2
V_2O_5	0.5	87.2	71.2	1.3	1.9	1.8	23.8	34.9
WO_3	1.5	9.2	57.2	42.1	0	0	0.7	8.1

a Water vapor was co-fed to the catalyst: toluene/NH_3/O_2/H_2O/He=1/10/4/10/24 (F = 49 mL min^{-1}).

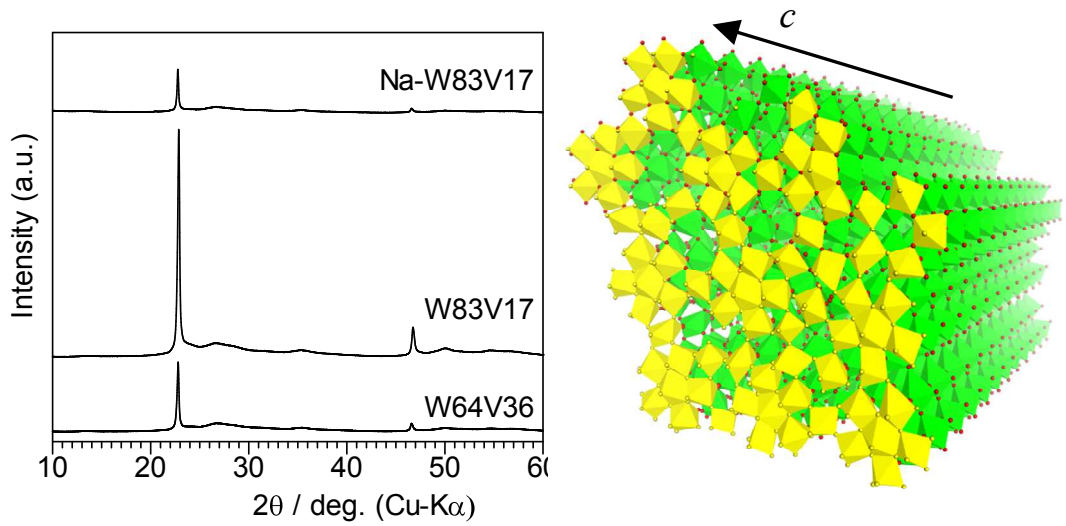

Fig. 1. XRD patterns (left) and polyhedral model (right) of microporous and layered W-V-O oxides. The top layer of the model is highlighted in yellow.

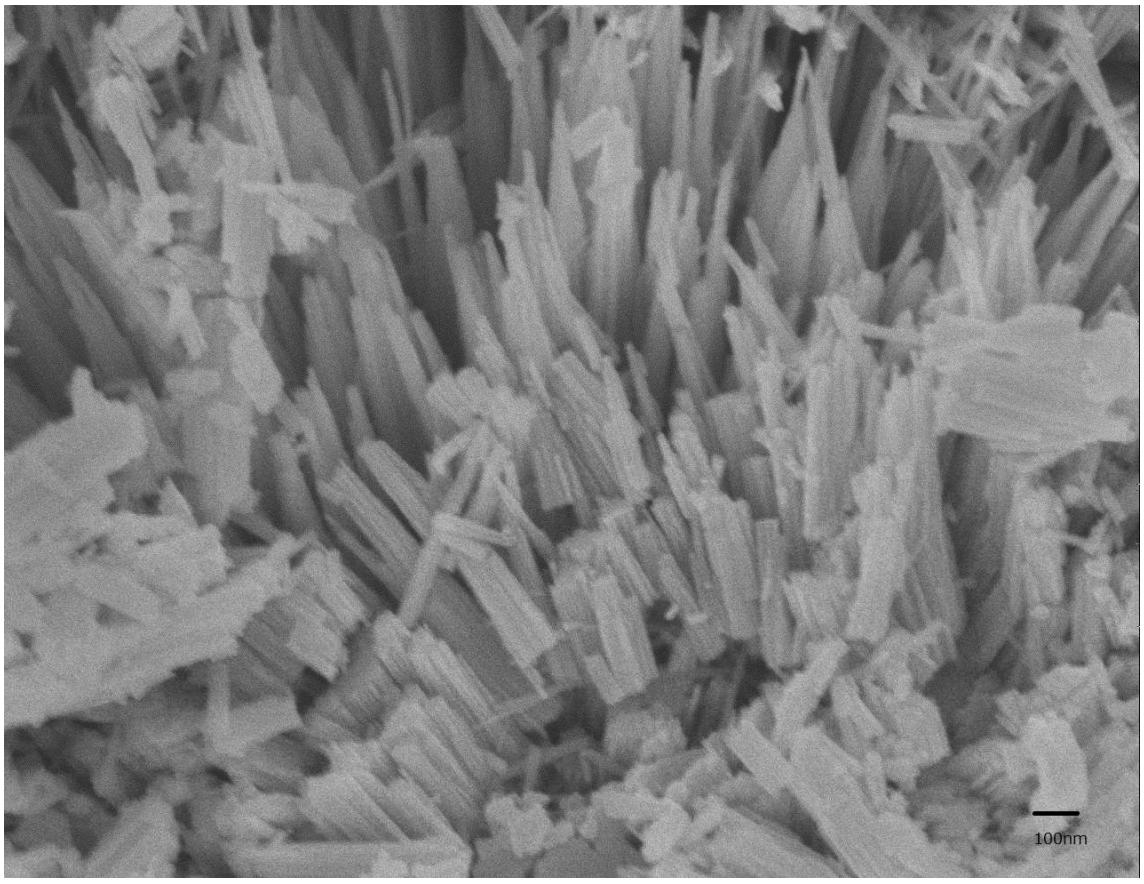

Fig. 2. SEM image of W83V17.

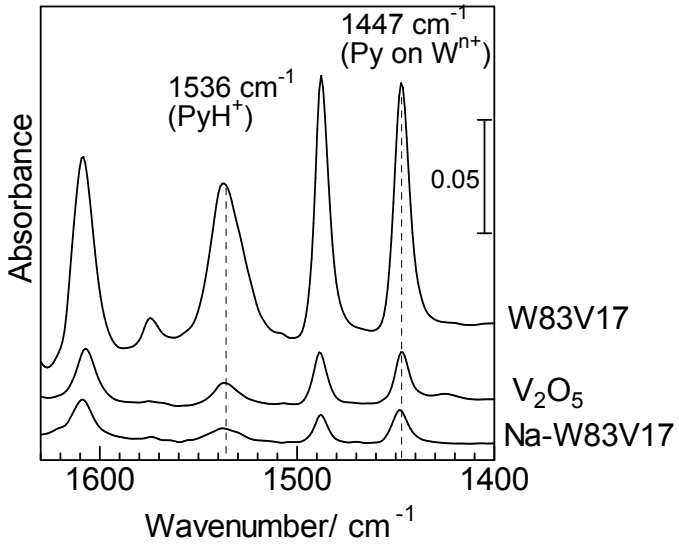

Fig. 3. IR spectra of pyridine adsorbed on the catalyst disc (38±1 mg) at 100 ˚C

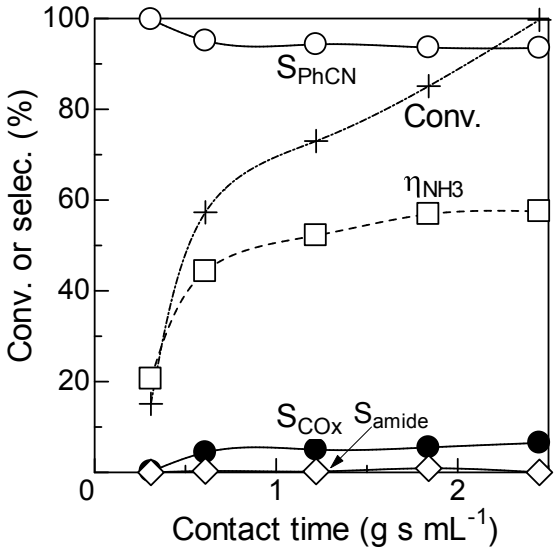

Fig. 4. Ammoxidation of toluene by W83V17 at different contact times (400 ˚C): conversion of toluene (+), selectivities of benzonitrile (○), benzamide (◇) and CO_x (●) and NH_3-efficiency, η_{NH3}, (□): toluene/NH_3/O_2/He=1/10/4/34.

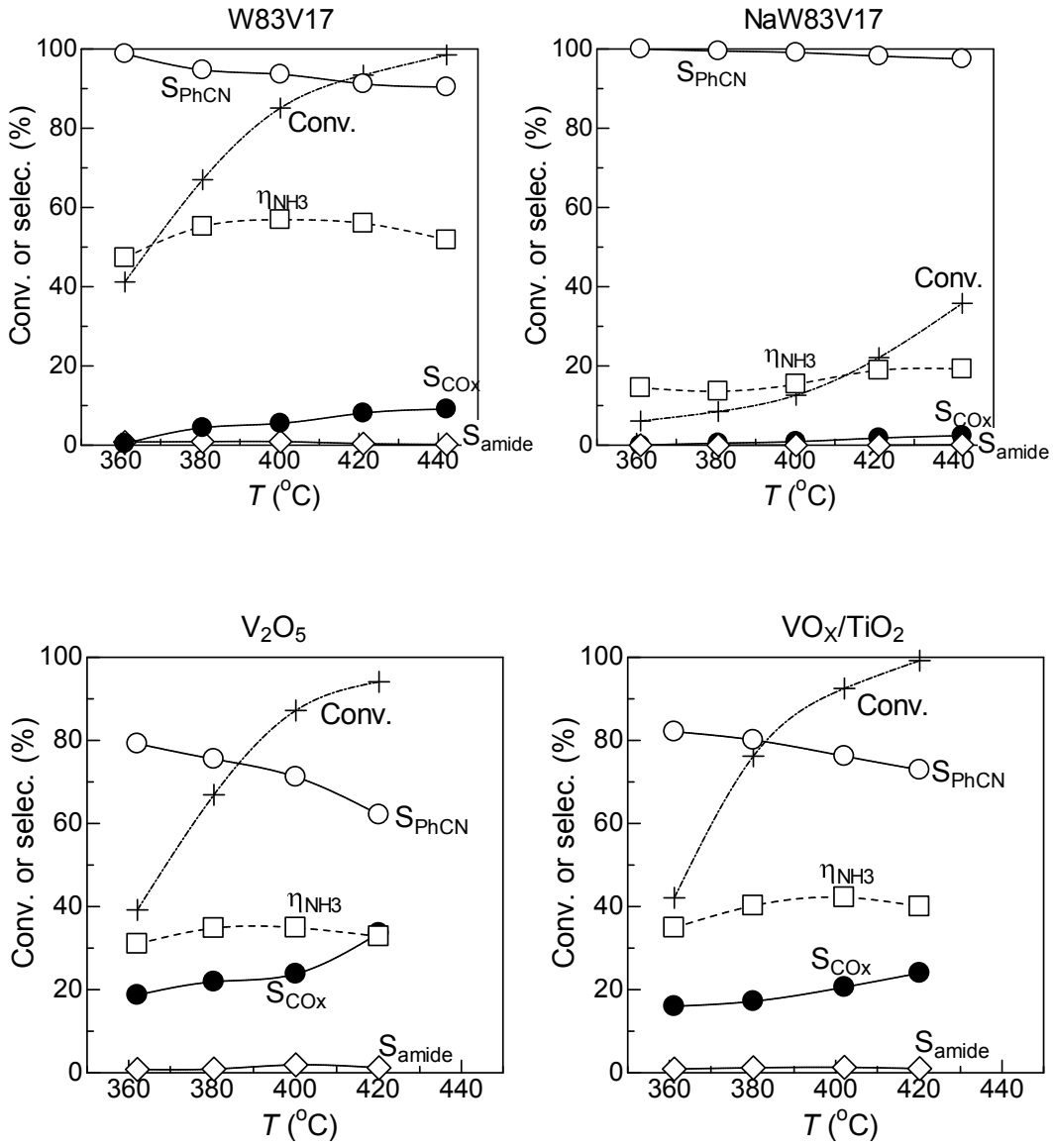

Fig. 5. Temperature dependence of the conversion of toluene (+), selectivities of benzonitrile (○), benzamide (◇) and CO_x (●) and NH_3-efficiency, η_{NH3}, (□) for ammoxidation of toluene by 1.5 g of W83V17: toluene/NH_3/O_2/He=1/10/4/34.

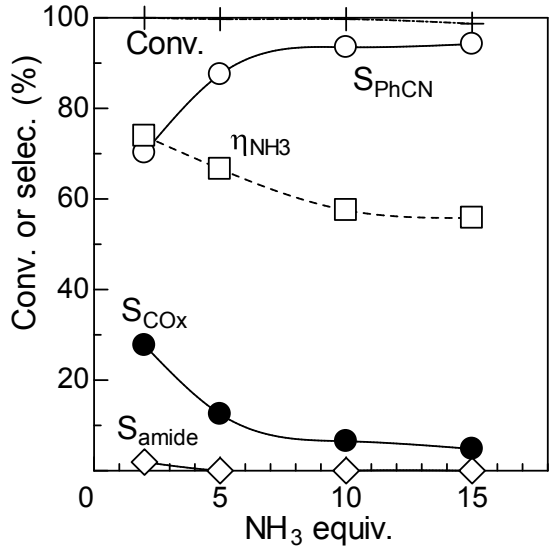

Fig. 6. Effect of the amount to NH_3 with respect to toluene on the conversion of toluene (+), selectivities of benzonitrile (○), benzamide (◇) and CO_x (●) and NH_3-efficiency, η_{NH3}, (□) for ammoxidation of toluene by 2 g of W83V17 at 400 ˚C: toluene/NH_3/O_2/He=1/10/4/34.

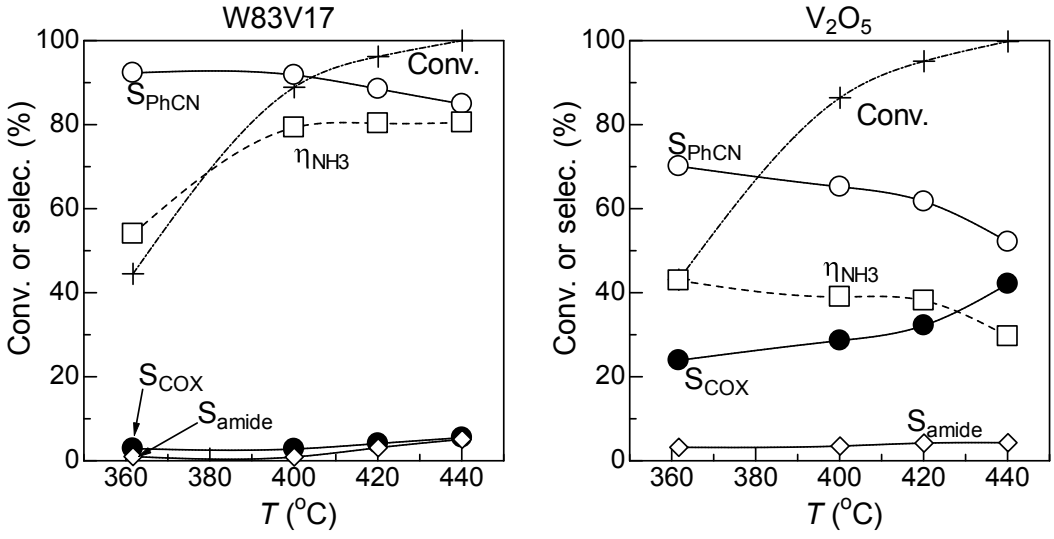

Fig. 7. Ammoxidation of toluene by 1.5 g of W83V17 and 0.5 g V_2O_5 in the low NH_3 concentration conditions (toluene/NH_3/O_2/He=1/5/4/39): conversion of toluene (+), selectivities of benzonitrile (○), benzamide (◇) and CO_x (●) and NH_3-efficiency, η_{NH3}, (□).

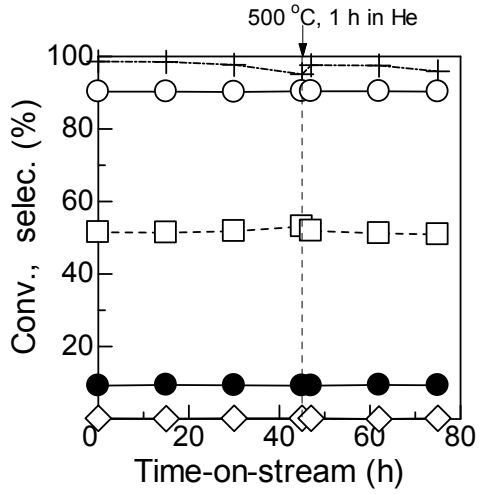

Fig. 8. Time course of ammoxidation of toluene by 1.5 g of W83V17 at 400 ˚C: conversion of toluene (+), selectivities of benzonitrile (○), benzamide (◇) and CO_x (●) and NH_3-efficiency, η_{NH3}, (□), toluene/NH_3/O_2/He=1/10/4/34. After 45 h of the reaction, the catalyst was heated at 500 ˚C for 1 h under He flow, followed by re-starting the ammoxidation reaction.

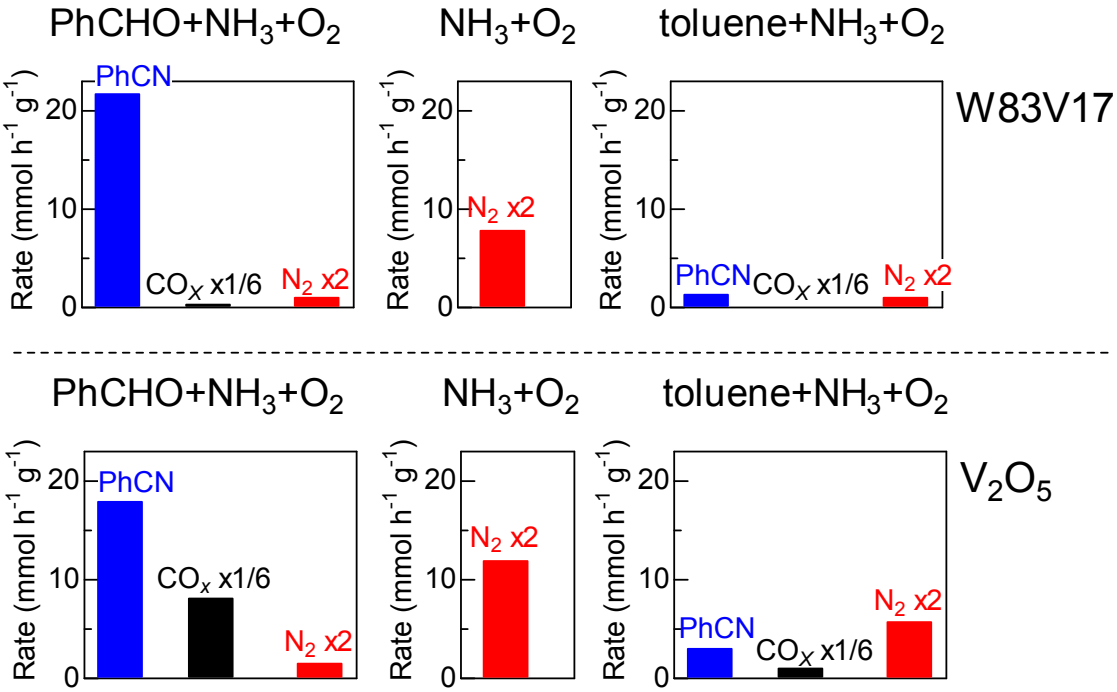

Fig. 9. Formation rates of PhCN, COx and N_2 for ammoxidation of benzaldehyde (left), oxidation of ammonia (center), and ammoxidation of toluene (right) by W83V17 (top) and V_2O_5 (bottom) at 400 ˚C.

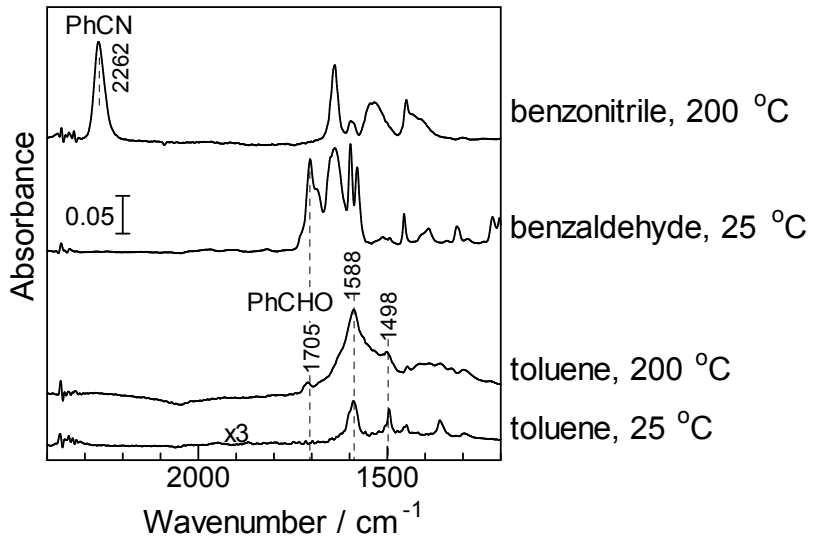

Fig. 10. IR spectra of adsorbed species on W83V17 at various temperatures.

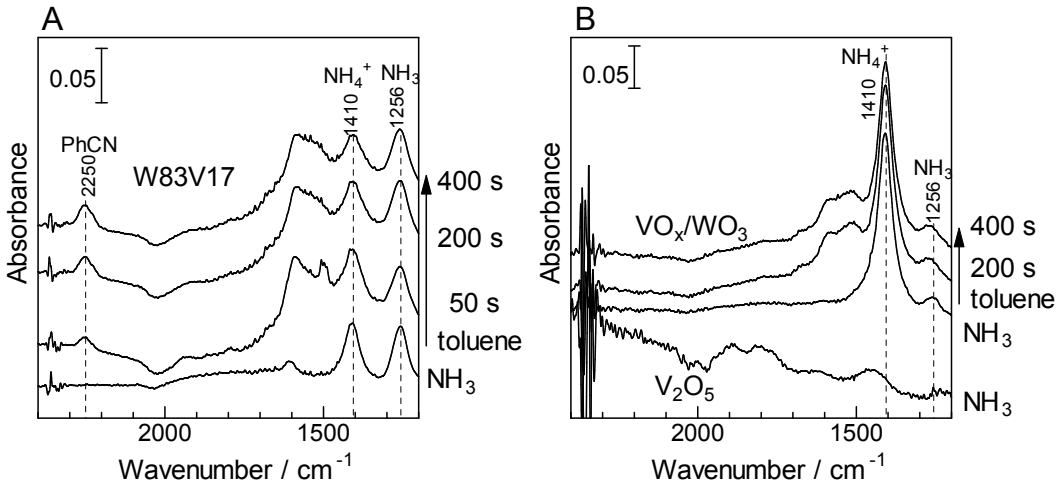

Fig. 11. IR spectra of adsorbed species on various catalyst discs (38±1 mg) during the reaction of adsorbed NH_3 species with toluene-derived species at 330 °C.

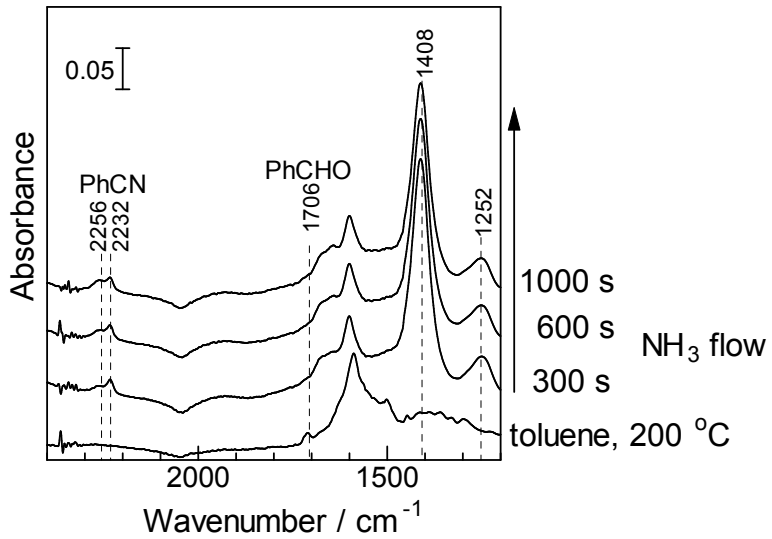

Fig. 12. IR spectra of adsorbed species on W83V17 during the reaction of toluene-derived surface species under flowing 2% NH_3/He at 200 °C.

Figure Captions

Fig. 1. XRD patterns (left) and polyhedral model (right) of microporous and layered W-V-O oxides. The top layer of the model is highlighted in yellow.

Fig. 2. SEM image of W83V17.

Fig. 3. IR spectra of pyridine adsorbed on the catalyst disc (38±1 mg) at 100 ˚C

Fig. 4. Ammoxidation of toluene by W83V17 at 400 ˚C at different contact times: conversion of toluene (+), selectivities of benzonitrile (○), benzamide (◇) and CO_x (●) and NH_3-efficiency, η_{NH3}, (□): toluene/NH_3/O_2/He=1/10/4/34.

Fig. 5. Temperature dependence of the conversion of toluene (+), selectivities of benzonitrile (○), benzamide (◇) and CO_x (●) and NH_3-efficiency, η_{NH3}, (□) for ammoxidation of toluene by 1.5 g of W83V17: toluene/NH_3/O_2/He=1/10/4/34.

Fig. 6. Effect of the amount to NH_3 with respect to toluene on the conversion of toluene (+), selectivities of benzonitrile (○), benzamide (◇) and CO_x (●) and NH_3-efficiency, η_{NH3}, (□) for ammoxidation of toluene by 2 g of W83V17 at 400 ˚C: toluene/NH_3/O_2/He=1/10/4/34.

Fig. 7. Ammoxidation of toluene by 1.5 g of W83V17 and 0.5 g V_2O_5 in the low NH_3 concentration conditions (toluene/NH_3/O_2/He=1/5/4/39): conversion of toluene (+), selectivities of benzonitrile (○), benzamide (◇) and CO_x (●) and NH_3-efficiency, η_{NH3}, (□).

Fig. 8. Time course of ammoxidation of toluene by 1.5 g of W83V17 at 400 ˚C: conversion of toluene (+), selectivities of benzonitrile (○), benzamide (◇) and CO_x (●) and NH_3-efficiency, η_{NH3}, (□), toluene/NH_3/O_2/He=1/10/4/34. After 45 h of the reaction, the catalyst was heated at 500 ˚C for 1 h under He flow, followed by re-starting the ammoxidation reaction.

Fig. 9. Formation rates of PhCN, COx and N_2 for ammoxidation of benzaldehyde (left), oxidation of ammonia (center), and ammoxidation of toluene (right) by W83V17 (top) and V_2O_5 (bottom) at 400 ˚C.

Fig. 10. IR spectra of adsorbed species on W83V17 at various temperatures.

Fig. 11. IR spectra of adsorbed species on various catalyst discs (38±1 mg) during the reaction of adsorbed NH_3 species with toluene-derived species at 330 °C.

Fig. 12. IR spectra of adsorbed species on W83V17 during the reaction of toluene-derived surface species under flowing 2% NH_3/He at 200 °C.